



A simple methodology to detect and quantify wind power ramps

Bedassa R. Cheneka¹, Simon J. Watson¹, and Sukanta Basu²

¹Faculty of Aerospace Engineering, Wind Energy Section, Delft University of Technology, Delft, The Netherlands

²Faculty of Civil Engineering and Geosciences, Delft University of Technology, Delft, The Netherlands

Correspondence: Bedassa R. Cheneka (b.r.cheneka@tudelft.nl)

Abstract.

Knowledge about the expected duration and intensity of wind power ramps is important when planning the integration of wind power production into an electricity network. How to detect and classify wind power ramps is not straightforward due to the large range of events that are observed and the stochastic nature of the wind. The development of an algorithm that can detect and classify wind power ramps is thus of some benefit to the wind energy community. In this study, we describe a relatively simple methodology using a wavelet transform to discriminate ramp events above stochastic variations using randomly shuffled wind power surrogates. To illustrate our approach, we used aggregated Belgian offshore wind power production data to characterise wind power ramps over a period of 10 days. We further illustrate the utility of the methodology by extracting distributions of ramp rates and their duration using two years of wind power production data. This brief study showed that there was a strong correlation between ramp rate and ramp duration, especially for up-ramps, that the majority of ramp events were less than 15 hours with a median duration of around eight hours and that ramps with a duration of more than a day were rare.

Keywords. Wavelet transform, Surrogate data, Ramps duration

1 Introduction

Rapid changes in wind speed cause ramps in wind power production of a wind farm. With plans to install a large amount of capacity in the North Sea, understanding swings in offshore wind farm power production will become important for wind farm and network operators to manage the integration of wind power into the electricity system. There is no accepted definition or classification of wind power ramps except that they are manifested in terms of a significant change in production over a relatively short time. In this paper, we propose a relatively simple technique based on wavelets and surrogates to detect wind power ramp events.

Wind power ramps are influenced by the dynamics of atmosphere-ocean systems which could be either mesoscale or synoptic-scale. Therefore, meteorological systems that evolve over time play a significant role in the occurrence of power ramps (Marquis et al., 2011). Low-pressure systems, cold fronts, low-level jets, thunderstorm outflows, and drylines can cause up-ramp (increasing wind) events (Sevlian and Rajagopal, 2013; DeMarco and Basu, 2018) whereas, down-ramp (decreasing wind) events occur due to the reduction or reversal of these physical processes (Ferreira et al., 2011). Short-duration (rapid)



power ramps are mainly influenced by mesoscale systems, whereas synoptic systems tend to be responsible for longer duration power ramps (Drew et al., 2018).

The detection of the duration and magnitude of wind power ramps has been explored by several scholars. Most of the studies set thresholds with respect to the rated power of the wind farm to detect wind power ramps. One such definition (Bossavy et al., 2010; Zhang et al., 2017) defines a ramp as a minimum change in wind farm output ΔP as a fraction of the rated wind power P_R of the wind farm over a maximum period of time (Δt). Different researchers consider different rates of change to define ramps, for example, Cutler et al. (2007) define a power ramp when there is a change in wind power production of 75% of P_R within a Δt of 3 hours or 65% of P_R within a Δt of 1 hour. In contrast, Bossavy et al. (2010) define a wind power ramp when there is a change in wind power of 50% of P_R over one hour. Other researchers such as Bianco et al. (2016) and Gallego-Castillo et al. (2015) use yet different percentage changes in wind power and time ranges to define wind power ramps. Clearly, this leads to some difference in what events are defined as wind power ramps.

There have been studies to detect power ramps without using any pre-defined change in wind power relative to rated power and time. An optimised swinging door algorithm was used by (Zhang et al., 2017) to extract ramps where the ramp definition parameters related to power change and timescale could be easily adapted. An optimal method to detect ramps based on scoring functions (Sevlian and Rajagopal, 2013) was used to detect ramps of varying lengths at a US wind farm. These authors used a piece-wise linear trending fit to remove short-term stochastic fluctuations. Moreover, it has recently been shown that the wavelet transform is a useful tool to detect wind power ramps (Hannesdóttir and Kelly, 2019; Ji et al., 2015; Gallego et al., 2014). The magnitude of the continuous wavelet transform (CWT) coefficient can be used to detect significant wind power ramps but discriminating wind power ramps from noise (i.e. incoherent stochastic variations) remains a challenge.

Even though there has been a significant body of work to detect wind power ramps, it is clear that there is no precise consensus as to the definition of a ramp. Indeed, it may be necessary to extract information about a range of power ramp events depending on the requirements of the wind farm operator or the utility. What is required is a robust method which can extract ramps of arbitrary magnitude and duration and to discriminate above the incoherent stochastic noise level. It is with this aim that we demonstrate how a wavelet transform can be used in conjunction with the generation of wind power surrogates to give a robust method for the detection of wind power ramps of varying magnitude and duration. We illustrate the methodology and its application using data from the Belgian offshore wind farm cluster. Firstly, we describe the methodology and illustrate its application using a ten-day period of data. Next, the sensitivity of the discrimination of ramps from natural stochastic variation is investigated using a longer period to generate the surrogate distributions. Finally, we show the utility of the approach in terms of characterising the distribution of ramp rates and their duration using two years of offshore wind-power data.

2 The wind farm data

The Belgian transmission system operator, Elia, makes available 15 minutes power output data for the aggregated fleet of Belgian onshore and offshore turbines (Elia, 2020). In this work, we have used offshore data over a period of two years from



2015-2016 when the combined Belgian offshore wind power capacity was 712 MW. For simplicity, the 15 minute values were normalised to the total capacity before analysis to create a time series of values $P(t)$.

60 3 Wavelet decomposition

The continuous wavelet transform (CWT) can be used to decompose a series of data using a mother wavelet function (φ) by varying its dilation and translation. A mother wavelet function with scale a and position b can be defined as (Mallat, 2009):

$$\varphi^{a,b}(t) = \varphi\left(\frac{t-b}{a}\right) \quad (1)$$

The CWT $W(a,b)$ of a signal $X(t)$ is produced by the convolution of the mother wavelet function over a range of scales and
65 positions:

$$W(a,b) = \frac{1}{\sqrt{a}} \int_{-\infty}^{\infty} X(t) \varphi\left(\frac{t-b}{a}\right) dt \quad (2)$$

A wavelet transform is thus able to localise the scales of a series of data in time which makes it a useful function to detect and characterise wind power ramps. We use the Daubechies level 1 (Haar) mother wavelet to decompose the time series of power values. This wavelet is useful to detect abrupt changes in a level which might be expected to occur during a ramp event.

70 Using values over a ten-day period, 27-Jan-2015 to 07-Feb-2015, taken from the Belgian offshore wind power data, a CWT was applied and the results are shown in Figure 1 comparing the original time series (top) with the corresponding CWT values (bottom). It can be seen that a high magnitude of W corresponds to a strong power ramp. Similar finding has been reported elsewhere (Gallego et al., 2014; Hannesdóttir and Kelly, 2019). However, what is not clear is what magnitude of W can be considered as a ramp above the incoherent stochastic variation in wind power. In the following section, we consider how to
75 discriminate ramps above such stochastic variation.

4 Discrimination of ramp events

Random shuffling is a technique to generate surrogate data from an original time series which preserves limited statistical properties of the original data, namely their distribution. However, it destroys the auto-correlation within a time series. Randomly shuffled surrogates have been used to test for non-linearity in a time series (Theiler et al., 1992). It has also been used to test for
80 stationarity in temporal data (Laurent and Doncarli, 1998; Davy and Godsill, 2002; Borgnat and Flandrin, 2009; Guarin et al., 2010; Borgnat et al., 2010). Furthermore, surrogates have been applied to discriminate gusts and other coherent structures from incoherent noise in high frequency wind speed data (Dunyak et al., 1998; Gilliam et al., 2000).

In Figure 2, we show an example surrogate based on the ten-day time series shown in the top plot of Figure 1. The top left plot of Figure 2 shows the randomly shuffled time series of normalised power values for which it is seen that any coherent

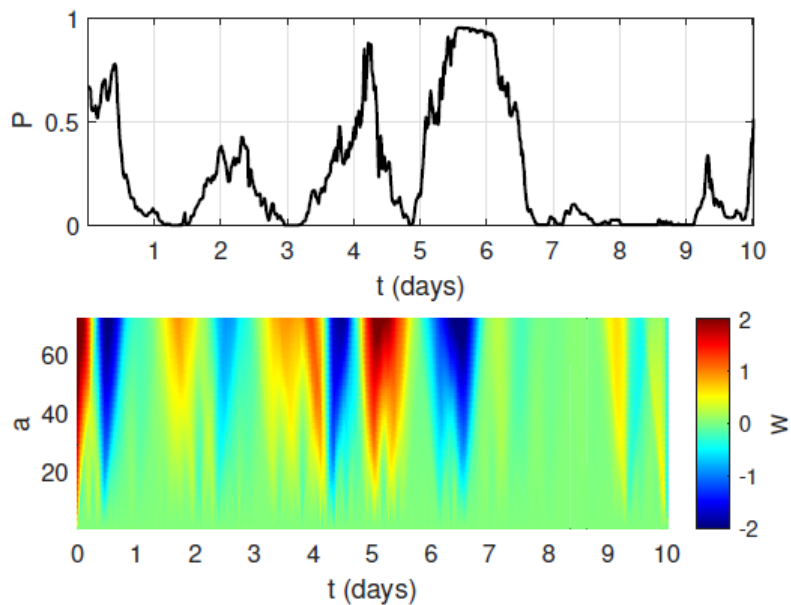


Figure 1. Top: aggregated normalised Belgian offshore wind power output over the period 27-Jan-2015 to 07-Feb-2015. Bottom: continuous wavelet transform of the wind power data using the Haar mother wavelet.

85 structure in the original data is destroyed and the time series resembles white noise. This is confirmed by the plot at the bottom right comparing the autocorrelation of the original time series with that of the surrogate. Finally, the plot at the bottom right of Figure 2 shows a continuous wavelet transform of the surrogate time series. It can be seen that the lower frequency (higher scale value) structure that was seen in the lower plot of Figure 1 has disappeared and the power in the transformed wavelet spectrum is much more distributed over all scales.

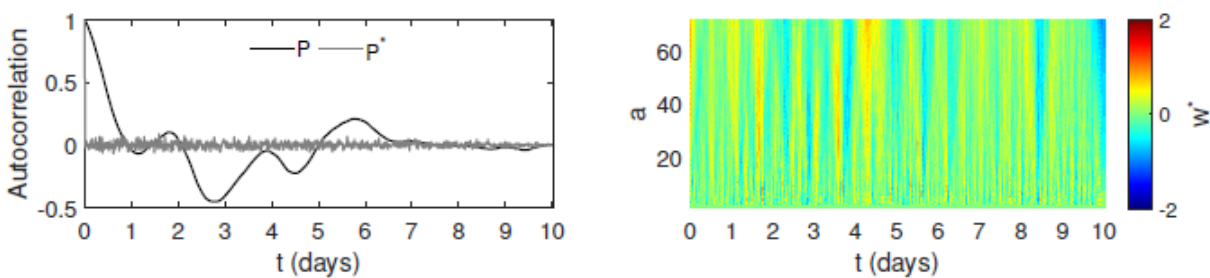


Figure 2. Left: the auto-correlations of the original wind power and the normalised wind power surrogate and; right: a CWT of the normalised wind power surrogate.



90 In order to test the hypothesis that the value of a wavelet coefficient represents a ramp event, we generate 100 such randomly shuffled surrogates of normalised wind power, $P_i^*(t)$, where $i = 1$ to 100, based on the ten days of data. For each surrogate time series, the CWT is generated to give a series of coefficients $W_i^*(a, b)$ as shown in Figure 2 (right). These are used to generate distributions of coefficient values (containing $100 \times b$ values) for each scale a , against which the CWT coefficient of the original, $W(a, b)$ can be compared. For instance, we have shown the distribution for W and W^* at the scale $a = 40$ for several thresholds at 90th, 95th, 98th and 99th percentile as shown in Figure 3 (top). Then, at the scale of $a = 40$, we have discriminated W with respect to W^* with the null hypothesis of 10%, 5%, 2% and 1% rejection levels.

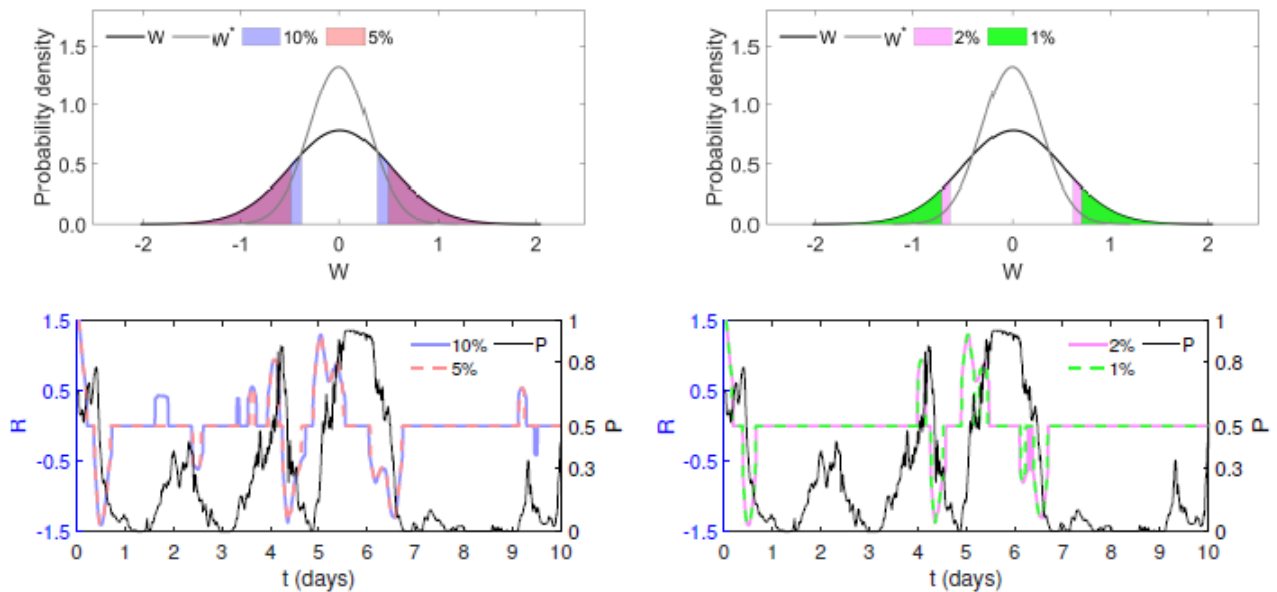


Figure 3. Top: the distribution of W and $W_T^*(a)$ shown at the scale ($a=40$). The shaded region show the 10%, 5%, 2% and 1% rejection levels. Bottom: the discriminated W at the scale ($a=40$) at each rejection levels and the normalized wind power.

Figure 3 - bottom - right shows that the rejection levels of 2% and 1% remove significant wind power ramps such as those occurring between the first and the fourth days; also the small ramps around the ninth and tenth days. Both null hypothesis rejection levels 10% and 5% seem realistic in detecting the wind power ramps as seen in Figure 3 - bottom - left. We extend the null hypothesis testing to all the scales of W . First, for each scale a , we compute a scale-dependent threshold $W_T^*(a)$ for a specific percentile (say 90th) by utilising the $|W_i^*(a, b)|$ values from all the surrogates. Next, if the value of $|W(a, b)|$ is greater than this threshold $W_T^*(a)$, then the null hypothesis is rejected at the 10% level and the event is assumed to be a wind power ramp. We repeat these steps for different percentiles (e.g., 90th, 95th, 98th and 99th).

Figure 4 shows the result of using this approach to discriminate the wind power ramps at each scale. The plot is similar to the bottom plot in Figure 1, but now values which do not satisfy the criterion to be considered as ramps have been removed



and are shown as white with different null hypothesis testing. Only the colour shaded values that satisfy the requirement to be considered as wind power ramps for different rejection levels are shown.

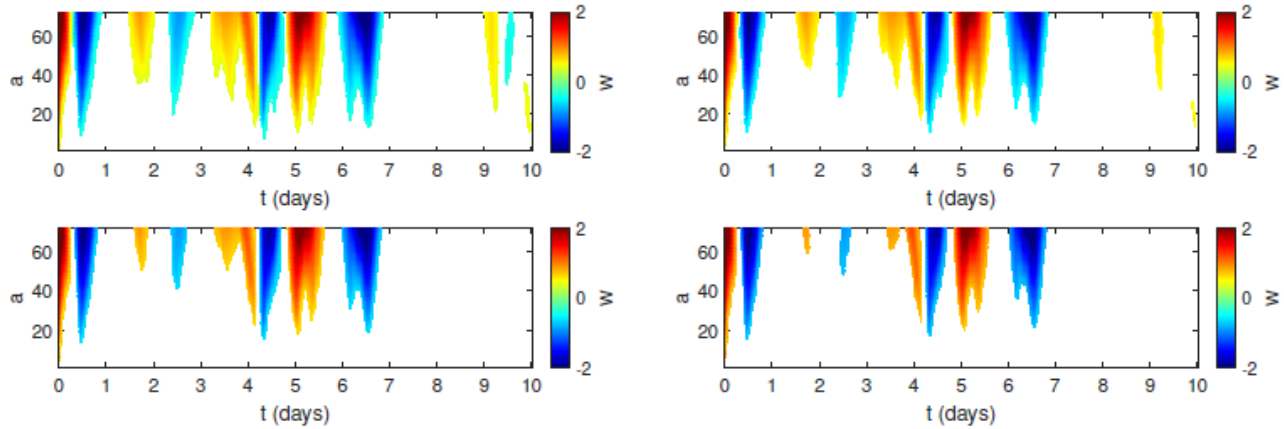


Figure 4. The CWT coefficients $W(a, b)$ of the normalized wind power discriminated against the distribution of $W_i^*(a, b)$ with the rejection levels at 10% (top-left), 5% (top-right), 2%(bottom-left) and 1% (bottom-right) significance level. The colour scale is blue (ramp-up events), red (ramp-down events) and white (no ramp).

It is then possible to sum $W(a, b)$ over all discriminated scales up to the maximum resolved, a_{max} at each time step, $t = b$ to calculate mean normalised power ramps, $R(t)$:

110

$$R(t = b) = \frac{1}{a_{max}} \sum_{a=1}^{a_{max}} W_R(a, b) \quad (3)$$

where:

$$\begin{aligned}
 W_R(a, b) &= W(a, b) && \text{when} && |W(a, b)| \geq W_T^*(a) \\
 W_R(a, b) &= 0 && \text{when} && |W(a, b)| < W_T^*(a)
 \end{aligned}$$

Figure 5 shows the original ten-day time series of offshore wind power values with the normalised ramp values, $R(t)$ superimposed. Power ramps are now clearly defined in terms of both timing and magnitude. The scale-dependent threshold value for a ramp, $W_T^*(a)$ could be adjusted by increasing the percentile value which is shown for the four rejection levels 10%, 5%, 2% and 1%. Comparing each of the rejection levels, the 10% null hypothesis test captures ramp duration and events. For instance, the ramp duration and events in days one to four; and days nine to ten are not well captured at the rejection levels of 5%, 2% and 1%. Therefore, hereafter in this paper, we consider the 10% to be sufficient to discriminate from incoherent stochastic fluctuations using the method of surrogates.

120

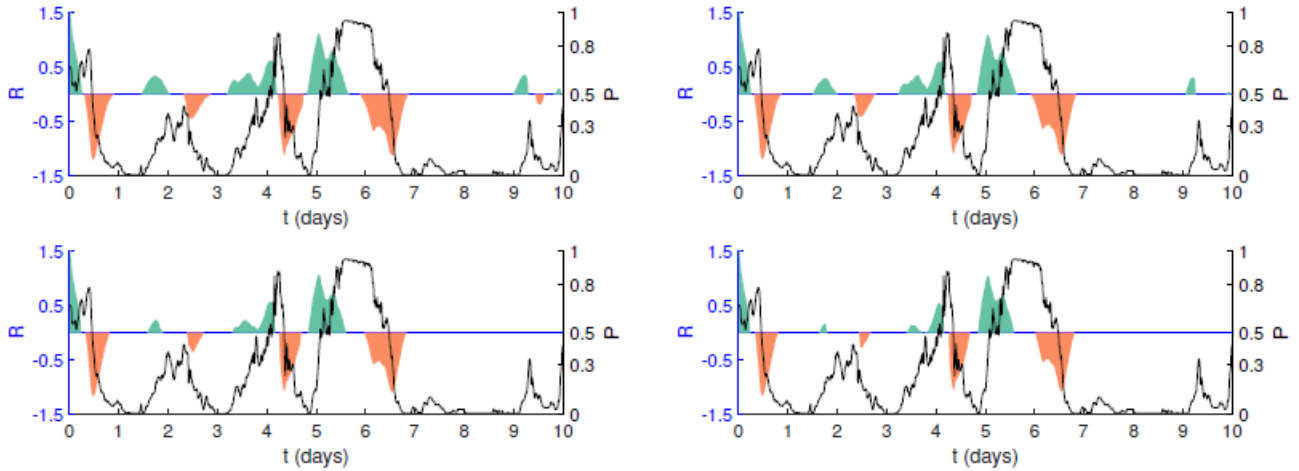


Figure 5. Normalised wind power ramps, $R(t)$ superimposed over the normalised wind power values $P(t)$ for the ten-day period for the null hypothesis test at the 10% (top-left), 5% (top-right), 2% (bottom-left) and 1% (bottom-right) significant level. Ramp-up events are shown in green and ramp-down events in orange.

5 Sensitivity to length of surrogate series

To test the generality of the technique, we consider further testing periods and increase the length of time for which the surrogate distributions are calculated. Three additional ten-day periods are selected and for each period, we examine the sensitivity of the results to the length of surrogate, namely: the same ten-day period and one calendar year of values encompassing the ten-day
 125 period. These cases are summarised in Table 1.

Table 1. Test periods and length of surrogate series used to detect and quantify ramps.

Test Period	Surrogate Period 1 (S_1)	Surrogate Period 2 (S_2)
28-Jan-2015–07-Feb-2015	Same as test period	2015
20-Nov-2015–30-Nov-2015	Same as test period	2015
27-Jan-2016–05-Feb-2016	Same as test period	2016
03-Nov-2016–13-Nov-2016	Same as test period	2016

As before, for each case, we generate 100 surrogates and the wavelet coefficients $W(a, b)$ are discriminated against the distributions generated using the two different surrogate periods in Table 1. The results are presented in Figure 6. It can be seen that once again, ramp periods are well discriminated from periods of incoherent stochastic variation. In addition, the results show no difference when using a longer period to generate the surrogates except at the very beginning and end of the time
 130 series. This is due to boundary effects inherent in using a convolution function which is integrated over all time and should

thus be disregarded in any comparison. The fact that the results show no differences when using an extended surrogate period confirms that the process is filtering out short-term incoherent fluctuations and that a ten-day period is sufficient to capture these.

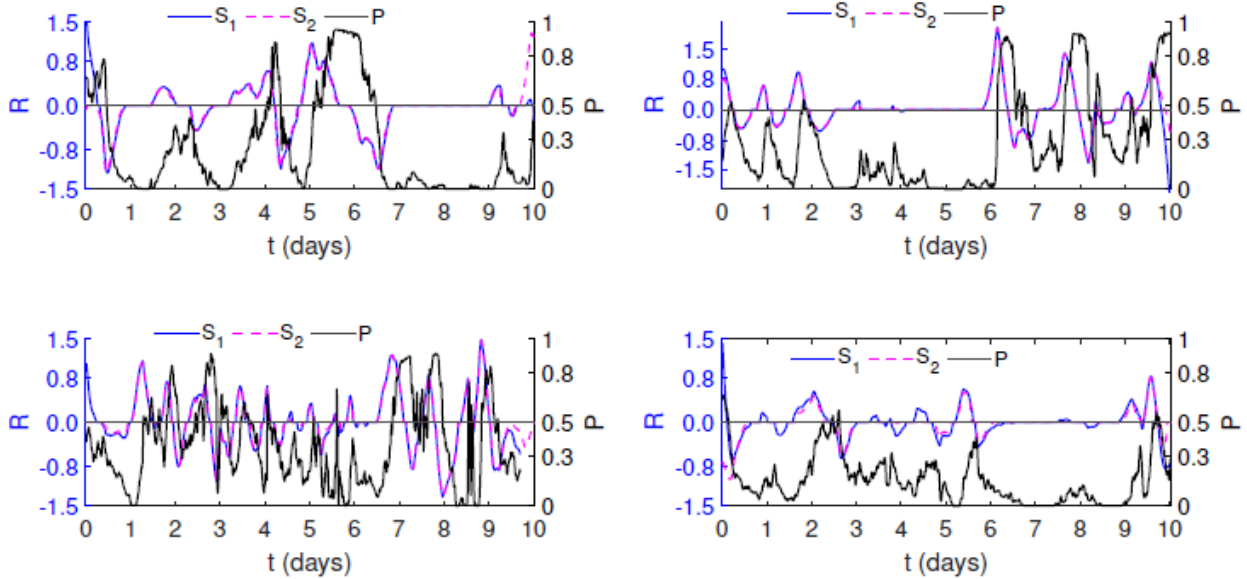


Figure 6. Normalised power ramps: (top-left) 28-Jan-2015–07-Feb-2015; (top-right) 20-Nov-2015–30-Nov-2015; (bottom-left) 27-Jan-2016–05-Feb-2016 and (bottom-right) 03-Nov-2016–13-Nov-2016. Normalised wind power is shown in gray color. The up-ramps and down-ramps derived using surrogates from the ten-day period (S_1) are shown in blue color; and the one-year surrogate period are shown as a magenta line (S_2).

6 Normalised ramp rates and duration

135 Finally, using the proposed methodology it is possible to quantify ramp rates and their duration in a straightforward way. We illustrate this using two years of the Belgian offshore wind power data for 2015–2016 and using the whole period to produce the surrogate distributions. Firstly, we generate a time series of normalised ramp rates. As can be seen in Figures 5 and 6, there are discrete periods of ramp-up and ramp-down events. For each ramp-up period k and ramp-down period l we calculate the average ramp-up rate, $R'_u(k)$ and average ramp-down rate $R'_d(l)$, respectively:

$$140 \quad R'_u(k) = \frac{\sum_{t=1}^{n_k} R(t)}{D(k)} \quad (4)$$

$$R'_d(l) = \frac{\sum_{t=1}^{n_l} R(t)}{D(l)} \quad (5)$$



where the n_k normalised power ramp-up values $R(t)$ are summed over the duration $D(k)$ of the k^{th} ramp-up event and the n_l normalised power ramp-down values $R(t)$ are summed over the duration $D(l)$ of the l^{th} ramp-down event. Distribution plots of ramp rates thus calculated as a function of duration are shown in Figure 7. The ramp-up and ramp-down event distributions are broadly similar in nature though there are some features of note:

- There is a strong correlation between the average normalised ramp rate and the duration of the ramp, though the correlation is stronger for the ramp-up events than the ramp-down events
- The majority of ramp durations are less than 15 hours with a median value of 8.25 hours for ramp-up events and 8.5 h for ramp-down events
- There are very few ramp events with a duration of longer than a day (24 hours)
- The wavelet transform resolves the longest wind power ramps duration of 32 hours

These results are based on one dataset for a limited two-year period. Clearly, further work is necessary to investigate the generality of the observations above. However, this short investigation does illustrate how wavelets can be used to investigate ramps rates, their duration and prevalence.

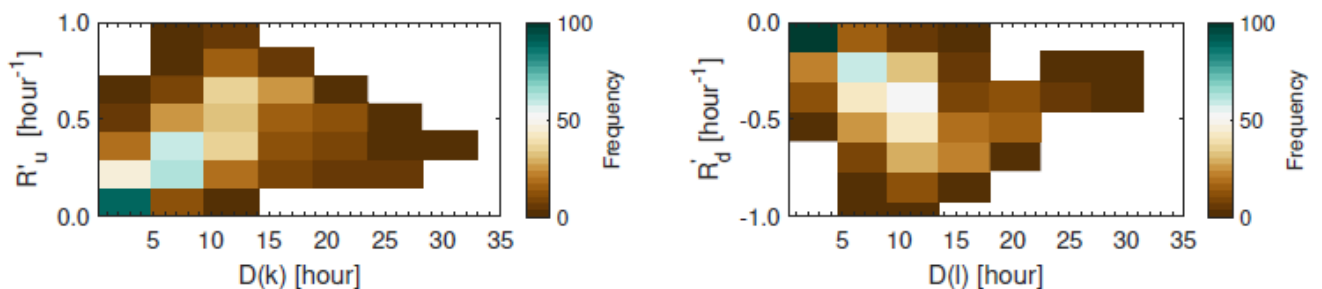


Figure 7. Distributions of normalised ramp rates as a function of duration for: (left) up-ramp rates, $R'_u(k)$ and (right) down-ramp rates, $R'_d(l)$.

155 7 Conclusions

The detection of wind power ramps is a challenge in terms of how to characterise their magnitude and duration and how to discriminate a ramp from incoherent stochastic fluctuations in wind power. In this paper, we have presented a relatively simple methodology based on a wavelet transform and the use of surrogates to discriminate and extract ramp events. Using data from the Belgian offshore wind farm cluster, we have illustrated the application of the methodology and have shown that a ten-day period is sufficient to discriminate coherent ramp events from incoherent fluctuations. Finally, we show the utility of the technique in characterising the distribution of ramp rates and their duration using two years of Belgian offshore wind power



data. Further work is required to apply the methodology to a broader range of sites and for longer periods to investigate the prevalence of different ramp rates and their duration. It might be expected that depending on the climatology of the site that this could differ; on the other hand, consistent trends may be apparent which could help operators in accommodating fluctuations within an integrated power system.

165

Data availability. The Belgian offshore wind power is publicly available at (Elia, 2020)

Author contributions. The results of this research are produced by Bedass R. Cheneka under the supervision of of Simon J. Watson and Sukanta Basu.

Competing interests. The authors declare that they have no conflict of interest.



170 References

- Bianco, L., Djalalova, I. V., Wilczak, J. M., Cline, J., Calvert, S., Konopleva-Akish, E., Finley, C., and Freedman, J.: A Wind Energy Ramp Tool and Metric for Measuring the Skill of Numerical Weather Prediction Models, *Weather and Forecasting*, 31, 1137–1156, <https://doi.org/10.1175/WAF-D-15-0144.1>, 2016.
- Borgnat, P. and Flandrin, P.: Stationarization via surrogates, *Journal of Statistical Mechanics: Theory and Experiment*, 2009, P01001, <https://doi.org/10.1088/1742-5468/2009/01/P01001>, 2009.
- 175 Borgnat, P., Flandrin, P., Honeine, P., Richard, C., and Xiao, J.: Testing Stationarity With Surrogates: A Time-Frequency Approach, *IEEE Transactions on Signal Processing*, 58, 3459–3470, <https://doi.org/10.1109/TSP.2010.2043971>, 2010.
- Bossavy, A., Girard, R., and Kariniotakis, G.: Forecasting Uncertainty Related to Ramps of Wind Power Production, in: *European Wind Energy Conference and Exhibition 2010, EWEC 2010*, vol. 2, pp. 9 pages – ISBN 9781617823 107, European Wind Energy Association, Warsaw, Poland, <https://hal-mines-paristech.archives-ouvertes.fr/hal-00765885>, 2010.
- 180 Cutler, N., Kay, M., Jacka, K., and Nielsen, T. S.: Detecting, categorizing and forecasting large ramps in wind farm power output using meteorological observations and WPPT, *Wind Energy*, 10, 453–470, <https://doi.org/10.1002/we.235>, 2007.
- Davy, M. and Godsill, S.: Detection of abrupt spectral changes using support vector machines an application to audio signal segmentation, <https://doi.org/10.1109/ICASSP.2002.5744044>, 2002.
- 185 DeMarco, A. and Basu, S.: On the tails of the wind ramp distributions, *Wind Energy*, 21, 892–905, 2018.
- Drew, D. R., Barlow, J. F., and Coker, P. J.: Identifying and characterising large ramps in power output of offshore wind farms, *Renewable Energy*, 127, 195–203, <https://doi.org/10.1016/j.renene.2018.04.064>, 2018.
- Dunyak, J., Gilliam, X., Peterson, R., and Smith, D.: Coherent gust detection by wavelet transform, *Journal of Wind Engineering and Industrial Aerodynamics*, 77-78, 467 – 478, [https://doi.org/https://doi.org/10.1016/S0167-6105\(98\)00165-2](https://doi.org/https://doi.org/10.1016/S0167-6105(98)00165-2), <http://www.sciencedirect.com/science/article/pii/S0167610598001652>, 1998.
- 190 Elia: Wind power generation, <https://www.elia.be/en/grid-data/power-generation/wind-power-generation>, 2020.
- Ferreira, C., J.Gama, Matias, L., Botterud, A., and Wang, J.: A Survey on Wind Power RAMP Forecasting, Tech. rep., Argonne National Laboratory (ANL), USA, 2011.
- Gallego, C., Cuerva, Á., and Costa, A.: Detecting and characterising ramp events in wind power time series, *Journal of Physics: Conference Series*, 555, 012 040, <https://doi.org/10.1088/1742-6596/555/1/012040>, 2014.
- 195 Gallego-Castillo, C., Cuerva-Tejero, A., and Lopez-Garcia, O.: A review on the recent history of wind power ramp forecasting, *Renewable and Sustainable Energy Reviews*, 52, 1148–1157, <https://doi.org/10.1016/j.rser.2015.07.154>, 2015.
- Gilliam, X., Dunyak, J., Doggett, A., and Smith, D.: Coherent structure detection using wavelet analysis in long time-series, *Journal of Wind Engineering and Industrial Aerodynamics*, 88, 183 – 195, [https://doi.org/https://doi.org/10.1016/S0167-6105\(00\)00048-9](https://doi.org/https://doi.org/10.1016/S0167-6105(00)00048-9), <http://www.sciencedirect.com/science/article/pii/S0167610500000489>, international Conference on wind Engineering, 2000.
- 200 Guarin, D., Orozco, A., and Delgado, E.: A new surrogate data method for nonstationary time series, 2010.
- Hannesdóttir, Á. and Kelly, M.: Detection and characterization of extreme wind speed ramps, <https://doi.org/10.5194/wes-2018-68>, 2019.
- Ji, F., Cai, X., and Zhang, J.: Wind power prediction interval estimation method using wavelet-transform neuro-fuzzy network, *Journal of Intelligent & Fuzzy Systems*, 29, 2439–2445, <https://doi.org/10.3233/IFS-151944>, 2015.
- 205 Laurent, H. and Doncarli, C.: Stationarity index for abrupt changes detection in the time-frequency plane, *IEEE Signal Processing Letters*, 5, 43–45, <https://doi.org/10.1109/97.659547>, 1998.



- Mallat, S.: A Wavelet Tour of Signal Processing, Elsevier, <https://doi.org/10.1016/B978-0-12-374370-1.X0001-8>, 2009.
- Marquis, M., Wilczak, J., Ahlstrom, M., Sharp, J., Stern, A., Smith, J. C., and Calvert, S.: Forecasting the Wind to Reach Significant Penetration Levels of Wind Energy, *Bulletin of the American Meteorological Society*, 92, 1159–1171, <https://doi.org/10.1175/2011BAMS3033.1>,
210 2011.
- Sevlian, R. and Rajagopal, R.: Detection and statistics of wind power ramps, *IEEE Transactions on Power Systems*, 28, 3610–3620, <https://doi.org/10.1109/TPWRS.2013.2266378>, 2013.
- Theiler, J., Eubank, S., Longtin, A., Galdrikian, B., and Farmer, J. D.: Testing for nonlinearity in time series: the method of surrogate data, *Physica D: Nonlinear Phenomena*, 58, 77–94, [https://doi.org/10.1016/0167-2789\(92\)90102-S](https://doi.org/10.1016/0167-2789(92)90102-S), 1992.
- 215 Zhang, J., Cui, M., Hodge, B.-M., Florita, A., and Freedman, J.: Ramp forecasting performance from improved short-term wind power forecasting over multiple spatial and temporal scales, *Energy*, 122, 528–541, <https://doi.org/10.1016/j.energy.2017.01.104>, 2017.